Contribution from the Division of Chemistry and Chemical Engineering, California Institute of Technology, Pasadena, California 91125, and Department of Chemistry, Columbia University, New York, New York 10027

Protein Surface Recognition and Covalent Binding by Chromium Nitrilotriacetate Complexes: Elucidation Using NMR and CD Spectroscopies

Jeffrey R. Bocarsly† and Jacqueline K. Barton*

Received July 24, 1991

New approaches to delineate sites of noncovalent and covalent binding by small metal complexes on a protein surface are described. The complexes employed are based on the chromium(III) nitrilotriacetate framework substituted with amino acid side chain groups. The protein examined is the well-characterized hen egg white lysozyme. Noncovalent binding location and mode have been studied by the technique of nuclear Overhauser effect quenching, along with paramagnetic relaxation experiments. These methods allow the elucidation of two major and two minor binding sites on the protein surface. The binding sites of greater intensity revolve around His-15 and active cleft residues Ala-107, Ile-98, and Trp-63 C2H, respectively. A comparison of the binding interaction as a function of the metal complex chelate ring substitutions suggests that the binding mode is modified by the side chain moiety; in particular, an aromatic–aromatic interaction between bound metal complex and aromatic residues on the protein surface is inferred. In addition to noncovalent interactions, the covalent labeling of coordinating protein side chains is examined. This is studied using circular dichroism to monitor the induction of vicinal dissymmetry in a symmetric metal complex through coordination of an amini acid side chain. These experiments indicate that aspartic acid residues near the sites of noncovalent association are labeled. As the sites of covalent labeling correlate well with the sites of noncovalent interaction, it is likely that the noncovalent binding influences the sites of covalent attachment.

The varied properties of transition-metal ions have made them attractive tools for the investigation of a wide variety of properties of proteins. Perhaps the most fundamental of these is the use of inorganic complexes to form heavy atom derivatives of proteins in order to enable the solution of protein X-ray structures.[1] However, in addition, transition-metal ions have been widely used as relaxation reagents to facilitate the assignment of biomolecular NMR spectra,[2] to map the electrostatic surface of proteins,[3] to study the geometry of enzyme binding sites,[4] and to separate protein mixtures chromatographically on the basis of variable abilities of chelating groups on the protein surface.[5] In addition to these structural investigations, transition-metal complexes have been shown to function as protein cross-linking reagents and protein tags,[6-9] to control the activity of suitably modified enzymes,[10,11] and to be probes for the properties of biological redox centers.[12,13] Finally, there has recently been strong interest in the utilization of transition metals and metal complexes as contrast agents in magnetic resonance imaging.[14-16]

Underlying these investigations are the questions of the recognition processes by which transition-metal complexes interact specifically with biological molecules. In each of the studies, the interaction of the metal complex with the biomolecular surface, whether noncovalent or covalent, plays a fundamental if implicit role in the progress of the chemistry. Recent work has already begun to delineate those factors which determine specific recognition of DNA sites;[17] however, relatively little work has been done in the same area with proteins. The principles behind the interaction of a given metal complex with a protein surface, or how a complex may be designed to target a specific surface structure, have not been detailed, nor have techniques been established to probe these recognition processes with high sensitivity.

Transition-metal complexes have several advantageous properties to offer the task of protein site recognition. First, the ligand binding properties of coordination complexes offer fixed geometries for ligand groups of biological interest. Second, the wide variety of ligand groups available allow a particular complex to be endowed with the range of interactions: electrostatic, hydrogen bonding, and various dipolar interactions. Finally, the transition-metal center, depending on the choice of metal and oxidation state, can have a variety of magnetic and spectroscopic properties, all of which may be useful design variables. This flexibility in design should permit the development of a potent array of inorganic probes for biomolecular structure.

As a system in which to start working out the principles of metal complex interactions with proteins, the chromium(III) nitrilotriacetate framework was selected. Among the advantages this system affords are the magnetic and spectroscopic properties of the chromium(III) center. We have demonstrated the utility of the paramagnetism of Cr(III) in assessing metal complex binding location and mode on a protein surface using the novel method of nuclear Overhauser effect (NOE) quenching spectroscopy along with classic paramagnetic broadening experiments.[18] Another useful spectroscopic advantage of this system is based on the ability to convert a symmetric metal complex into a dissymmetric chromophore, through the coordination of a ligand bearing an asymmetric atom.[19,20] This type of dissymmetry, known as vicinal dissymmetry, can be induced by an asymmetric center on a ligand several bonds away from the donor atom. Thus, the coordination of an amino acid side chain to a transition-metal center can be readily explored through the consequent vicinal dissymmetry, using circular dichroism (CD) spectroscopy.[21-23] Using these techniques,

* To whom correspondence should be addressed.
† Present address: Department of Chemistry, University of Connecticut, Storrs, CT 06269.

(1) McPherson, A. *Preparation and Analysis of Protein Crystals*; John Wiley and Sons: New York, 1982; Chapter 6.
(2) Campbell, I. D.; Dobson, C. M.; Williams, R. J. P.; Xavier, A. V. *J. Magn. Reson.* **1973**, *11*, 172-181.
(3) Tam, S.-C.; Williams, R. J. P. *Struct. Bonding (Berlin)* **1985**, *63*, 103-151.
(4) Mildvan, A. S.; Rosevear, P. R.; Granot, J.; O'Brien, C. A.; Bramson, H. N.; Kaiser, E. T. *Methods Enzymol.* **1983**, *99*, 93-119.
(5) Hemdan, E.; Zhao, Y.-J.; Sulkowski, E.; Porath, J. *Proc. Natl. Acad. Sci. U.S.A.* **1989**, *86*, 1811-1815.
(6) Peerey, L. M.; Kostic, N. M. *Inorg. Chem.* **1987**, *26*, 2079-2083.
(7) Ratilla, E. M. A.; Brothers, H. M.; Kostic, N. M. *J. Am. Chem. Soc.* **1987**, *109*, 4592-4599.
(8) Chen, J.; Kostic, N. M. *Inorg. Chem.* **1988**, *27*, 2682-2687.
(9) Brothers, H. M.; Kostic, N. M. *Inorg. Chem.* **1988**, *27*, 1761-1767.
(10) Corey, D. R.; Schultz, P. G. *J. Biol. Chem.* **1989**, *264*, 3666-3669.
(11) Higaki, J. N.; Haymore, B. L.; Chen, S.; Fletterick, R. J.; Craik, C. S. *Biochemistry* **1990**, *29*, 8582-8586.
(12) Yocom, K. M.; Shelton, J. B.; Shelton, J. R.; Schroeder, W. A.; Worosila, G.; Isied, S. S.; Bordignon, E.; Gray, H. B. *Proc. Natl. Acad. Sci. U.S.A.* **1982**, *79*, 7052-7055.
(13) Farver, O.; Pecht, I. *Coord. Chem. Rev.* **1989**, *95*, 17-45.
(14) Bydder, G. M. In *Practical NMR Imaging*; Foster, M. A., Hutchison, J. M. S., Eds.; IRL Press: Oxford, 1987; Chapter 7.
(15) Lauffer, R. B. *Chem. Rev.* **1987**, *87*, 901-927.
(16) Larsen, S. K.; Jenkins, B. G.; Memon, N. G.; Lauffer, R. B. *Inorg. Chem.* **1990**, *29*, 1147-1152.
(17) Barton, J. K. *Science* **1986**, *233*, 727-734.
(18) Bocarsly, J. R.; Barton, J. K. *Inorg. Chem.* **1989**, *28*, 4189-4190.
(19) Job, R. *Stereochemistry of Optically Active Transition Metal Compounds*; The American Chemical Society: Washington, DC, 1980; pp 273-288.
(20) Hawkins, C. J. *Absolute Configuratioin of Metal Complexes*; Wiley-Interscience: New York, 1971; Chapter 5.

0020-1669/92/1331-2827$03.00/0

Scheme I

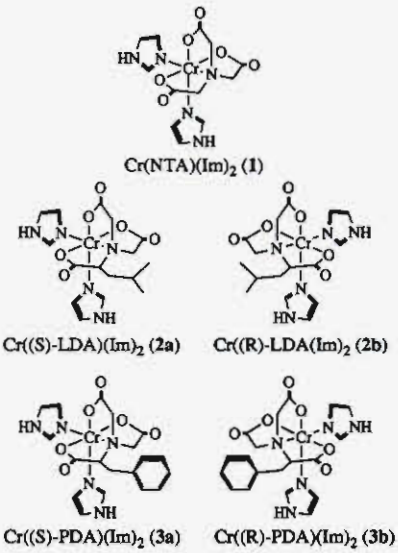

both the noncovalent binding of metal complex to protein surface and the covalent linkages which may be formed have been investigated.

In addition to these spectroscopic aspects, the chromium(III) nitrilotriacetate system has several useful structural features. First, the nitrilotriacetate ligand set contains three coordinated carboxylates which form a discrete hydrogen-bonding surface comprising one domain of the molecule. Next, the ligand framework can be relatively easily derivatized with amino acid side chain moieties, allowing the addition of varied recognition elements. Finally, the tetradentate nitrilotriacetate system allows two open cis coordination sites where monodentate ligands which can be labilized may be placed, allowing substitution of coordinating protein groups in the primary coordination sphere of the metal ion. These structural aspects of the complexes used in this study have been fully characterized.[24]

As substitutions on the nitrilotriacetate framework, aliphatic (leucine) and aromatic (phenylalanine) moieties were selected. These substitutions allow the examination of the role of the weaker biological interactions, such as steric, hydrophobic, and weakly polar aromatic interactions in the binding of these uncharged coordination complexes to the protein surface. Both the (*R*)- and (*S*)-amino acids may be used in the synthesis of these compounds, allowing metal complex chirality to become another variable in the binding interactions. The cis coordination sites unfilled by the nitrilotriacetate donor set were filled with imidazole ligands, which can potentially act as hydrogen bond donors. The family of complexes appear in Scheme I.[25]

As the protein target for these complexes, hen egg white (HEW) lysozyme[26] was chosen. Lysozyme, a bacteriolytic enzyme which hydrolyzes the β-(1→4) glycosidic linkage of *N*-acetylmuramic acid containing saccharides, has the advantage of a high-resolution X-ray structure,[27] an almost fully assigned ^{1}H NMR spectrum,[28] and a known propensity for binding nonsubstrate molecules. These characteristics suggested that lysozyme would make a useful target for initial metal complex–protein binding studies. HEW lysozyme

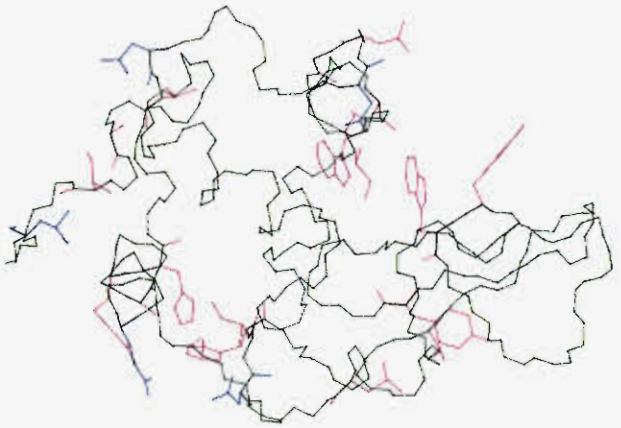

Figure 1. Model of hen egg white lysozyme based on the crystallographic coordinates deposited in the Brookhaven Protein Data Base. The peptide backbone of the protein is shown in green. Residues involved in the four regions of interaction are shown in red (see text). Clockwise from lower left, these include the His-15 site (Ala-11, Arg-14, His-15, Ile-88, Thr-89, and Phe-3); the Val-120 site (Val-120, Ala-122, and Ile-124); the active cleft site (Trp-62, Trp-63, Ile-98, Asn-103, Gly-104, Ala-107, and Trp-108); and the Leu-84 site (Thr-43, Tyr-53, and Leu-84). Highly solvent-exposed carboxylate side chains are shown in blue, including (clockwise from bottom) Asp-87, Glu-7, Leu-129, Asp-119, and Asp-101.

is shaped roughly like a prolate spheroid, with a deep, wedge-shaped cleft on one side. This cleft, the active cleft, contains six binding subsites (labeled A–F) into which a hexasaccharide may bind. Figure 1 shows a schematic of the structure of lysozyme with relevant surface residues targeted by the chromium complexes delineated.

As this work illustrates, the characteristics of transition-metal complexes permit a wide variety of interactions with the protein surface, ranging from noncovalent to covalent, and their spectroscopic features facilitate the investigation of binding type, location, and mode. An elucidation of the factors involved in the broad range of interactions of complex with protein, and how they may interrelate, constitutes the initial step toward understanding how inorganic drugs and site-specific labels may be rationally designed.

Experimental Section

Spectroscopy. NMR experiments were performed at 400 MHz on a Varian VXR-400 system equipped with an Oxford magnet. Circular dichroism spectra were recorded on a Jasco 500A spectrophotometer, and electronic spectra were recorded on a Varian DMS-300 UV–visible spectrophotometer. Atomic absorption determinations were performed on a Varian AA-875 atomic absorption spectrophotometer equipped with a GTA-95 graphite tube atomizer.

NMR Studies of Complex Binding. Grade I HEW lysozyme (purchased from Sigma) was exhaustively dialyzed against water at pH 3.0 (HCl) at 4 °C. The solution was then frozen, lyophilized, and stored desiccated at −20 °C until used. In a typical experiment, a weighed amount of lysozyme was dissolved in D_2O, and was then kept in an 80 °C water bath for 10 min to fully exchange all labile protons. After cooling, 2 mg of DSS was added as internal standard and the pH was adjusted with DCl/NaOD until the pH meter reading was 3.8. The protein concentration was then monitored by ultraviolet absorbance, using $\epsilon_{280} = 37\,600\ M^{-1}\ cm^{-1}$.[26] Protein concentrations were approximately 3 mM. A stock solution of metal complex was then made up in CD_3OD. This solvent was used as the metal complexes are both more soluble and less reactive with solvent in methanol. Metal complex stock solution concentrations were such that methanol was <2% of the total volume of the final protein–metal complex solution, which should not perturb protein conformation.[29] An NMR tube was then charged with 1.00 mL of protein solution and an amount of complex stock solution so that the desired protein–chromium complex ratio was achieved. NMR samples were then inserted into a Varian VXR-400 system magnet and equilibrated at 35 °C. For paramagnetic broadening experiments, the data were acquired with the sample spinning. The HDO peak was suppressed by a 2-s irradiation pulse prior to acquisition; a 0.5-s acquisition time

(21) Hawkins, C. J.; Lawson, P. J. *Inorg. Chem.* **1970**, *9*, 6–11.
(22) Frelek, J.; Perkowska, A.; Snatzke, G.; Tima, M.; Wagner, U.; Wolff, H. P. *Pure Appl. Chem.* **1985**, *57*, 441–451.
(23) Frelek, J.; Majer, Z.; Perkowska, A.; Snatzke, G.; Vlahov, I.; Wagner, U. *Spectrosc. Int. J.* **1983**, *2*, 274–295.
(24) Bocarsly, J. R.; Chiang, M. Y.; Bryant, L.; Barton, J. K. *Inorg. Chem.* **1990**, *29*, 4898–4907.
(25) Abbreviations: NTA = nitrilotriacetate; LDA = leucine-*N*,*N*-diacetate; PDA = phenylalanine-*N*,*N*-diacetate; Im = imidazole.
(26) Imoto, T.; Johnson, L. N.; North, A. C. T.; Phillips, D. C.; Rupley, J. A. In *The Enzymes*; Boyer, P. D., Ed.; Academic Press: New York, 1972; Chapter 21.
(27) Blake, C. C. F.; Koenig, D. F.; Mair, G. A.; North, A. C. T.; Phillips, D. C.; Sarma, V. R. *Nature* **1965**, *206*, 757.
(28) Redfield, C.; Dobson, C. M. *Biochemistry* **1988**, *27*, 122–136.
(29) Lehmann, M. S.; Mason, S. A.; McIntyre, G. J. *Biochemistry* **1985**, *24*, 5862–5869.

proved to be sufficient, as the narrowest peak in the spectrum was >2 Hz full width at half-height. Usually, 2–4 steady-state pulses preceded collection of transients. A total of 100–200 transients were collected (using a block size of either 100 or 200 transients) and transformed after resolution enhancement. In the case of the NOE quenching experiments, the sample was not spun. A 1-s irradiation pulse was used on the peak of interest, followed by an acquisition time of 0.5 s. Only resonances which the paramagnetic broadening experiments had shown not to be affected by the presence of chromium complex were chosen for irradiation. A total of 1200 transients were acquired per irradiation with interleaving (block size 40 transients). Spectra were then processed, usually with a 2-Hz line-broadening function. NOE spectra are presented as positive peaks for convenience; however, all lysozyme NOEs are negative. NOE enhancements are presented as percentages calculated from the peak area ratios of NOE peak to irradiated peak.

Synthesis of the Complexes. Complexes **1–3** were prepared and characterized as previously described.[24]

Model Complex Preparation. Amino acids were purchased from Sigma or Bachem, Inc., with both amine and α-carboxylate protection. Amine protecting groups were either *N*-acetyl or *N*-*tert*-butyloxycarbonyl (*N*-*t*-Boc) protection; α-carboxylates were protected as methyl, ethyl, or benzyl esters. Amino acids used for model complex synthesis were *N*-(*tert*-butyloxycarbonyl)-L-aspartic acid α-benzyl ester, *N*-(*tert*-butyloxycarbonyl)-L-glutamic acid α-benzyl ester, *N*-(*tert*-butyloxycarbonyl)-L-leucine, *N*-(*tert*-butyloxycarbonyl)-L-histidine α-methyl ester, and *N*-acetyl-L-tryptophan α-ethyl ester. Model complexes prepared and characterized were Cr(NTA)(Im)(*N*-(*tert*-butyloxycarbonyl)-L-aspartic acid α-benzyl ester) (**1a**), Cr(NTA)(Im)(*N*-(*tert*-butyloxycarbonyl)-L-glutamic acid α-benzyl ester) (**1b**), and Cr(NTA)(Im)(*N*-(*tert*-butyloxycarbonyl)-L-leucine) (**1c**).

All reactions were performed under mild conditions as follows: approximately 0.23–0.27 mmol of metal complex and 0.70–0.80 mmol of protected amino acid were combined in 5.0 mL of methanol. The solution was then stored at ambient temperature in the dark for 7–9 days. Solutions were monitored by following the buildup of the CD signal. At the end of the reaction period, a CD spectrum of the solution was taken, and the reaction mixture was evaporated to low volume in a stream of dry nitrogen and chromatographed on a 1- × 2-cm column packed with Sephadex A-25 QAE anion exchanger loaded in neat methanol. A band which appeared to be the same color as starting material was eluted with neat methanol; this band produced no CD signal in any of the reactions. A violet to purple band, which did not move under methanol elution, was then eluted with 50 mM LiBr in methanol. In all cases, this band contained optically active material which gave a CD signal identical to that of the solution prior to chromatography. This second band was concentrated in a stream of dry nitrogen (where necessary), and the visible and CD spectra were then measured. CD spectra were generally (although not exclusively) recorded by signal averaging eight scans taken at 100 nm/min scan speed. Smoothing was performed by truncating the Fourier transform of the spectrum with an empirically determined rectangular box function followed by retransformation into the wavelength domain. The concentration of chromium was determined by evaporating the methanol solutions to dryness in a stream of dry nitrogen, followed by alkaline hydrogen peroxide oxidation of the chromium to chromate ion,[30] using $\epsilon_{372} = 4815\ M^{-1}\ cm^{-1}$,[31] to allow calculation of ε and of Δε. FAB mass spectra of the solutions, both positive and negative ion, were measured in a 3-nitrobenzyl alcohol matrix to characterize the products.

Protein Labeling Reactions. Initial labeling reactions of lysozyme with **1** were studied as functions of the protein to metal complex ratio and reaction pH. First, buffered and unbuffered blanks containing metal complex without protein were run in order to ensure that no CD developed in the absence of chiral reactants. In no case did any blank reaction produce any measurable CD signal. Reactions with protein were then conducted as follows. Lysozyme was prepared as described above. An amount of protein sufficient for 1.5 mL of a 3–4 mM solution per reaction was dissolved in water. The pH of the solution was then adjusted to the desired value using HCl or NaOH. The protein concentration was then monitored by UV absorbance. The solution was then syringe filtered into a cuvette containing the desired amount of metal complex. The cuvette was then incubated with stirring at 35 °C for the desired amount of time; CD spectra were taken at appropriate intervals. Initial experiments were conducted using both buffered (phosphate–citrate buffers) and unbuffered protein solutions. Both buffered and unbuffered protein labeling reactions produced the same CD spectrum; however, the buffered solutions produced less intense spectra. This may be due either to the presence of polarizable anions from the buffer, which are known to affect rotational strength,[20] or to the increase in ionic strength in the buffered solutions. Insofar as the protein proved completely stable in the absence of buffer, most reactions were carried out in unbuffered solutions. Full labeling, as indicated by an increase in the CD signal to a maximum, was achieved after 20 h of reaction at 35 °C using a 5:1 metal complex to protein ratio. After the reaction was terminated, the labeled protein was purified by dialysis to remove unreacted chromium complex. The labeled protein was stored desiccated at −20 °C after lyophilization.

Determination of Metal Binding Stoichiometry. A solution of lysozyme was fully labeled as indicated by CD, dialyzed, and lyophilized. A weighed amount of fully labeled protein (0.0536 g) was dissolved in 1.50 mL of water. CD and visible spectra were then recorded. Dilutions were then made up, and the metal ion concentrations of these dilutions were measured by standard atomic absorbtion techniques. The absorption of each dilution was measured three times, and the average was compared with a standard absorption curve. The average chromium concentration was compared to the concentration of labeled protein as determined by weighing. The final concentration of protein was found using a molecular weight adjusted for the mass of the labels, from which a stoichiometry was calculated.

Potentiometric Titration of Labeled Lysozyme. A solution of labeled lysozyme in water (~1 mL) was made up, and the spectrum (either visible or CD) was recorded. The solution was titrated by addition of microliter volumes of ~0.1 M $HClO_4$, so that the change in protein concentration during titration was negligible. The pH of the solution was then measured, followed by visible or CD spectroscopy.

Results

NMR Studies of Binding Location and Mode. Initial paramagnetic broadening experiments showed that the interactions of the five metal complexes with lysozyme were broadly similar to each other both in their regions of specific interaction and in the extent of their nonspecific interactions. A similarity in specific metal complex–protein interactions for **1–3** is expected, as the interactions common to all the complexes (e.g., hydrogen bonding by the nitrilotriacetate framework) are both higher in energy and more numerous than the side chain interactions (i.e., steric or weakly polar interactions) specific to any one complex. These initial relaxation results were used to select resonances which were both unbroadened in the presence of metal complex and suitable candidates for irradiation in NOE quenching experiments. The NOE quenching technique and the paramagnetic broadening data were then used to identify binding sites. These experiments demonstrated the presence of two strong sites of interaction on the protein surface which are specific and at least two areas of weaker interaction.[32]

The His-15 Site. The first strong site, which evidences itself most clearly at the His-15 δ-CH resonance at δ 8.96 ppm, is an interaction that is strikingly dependent on the structure of the metal complex. Figure 2 shows the effect on this resonance of a 5:1 ratio of lysozyme to metal complex. The interaction is dependent on side chain stereochemistry and not on side chain type; the overall order of interaction at this resonance is **2a** ≈ **3a** > **1** > **2b** ≈ **3b**.

Further light may be shed on the nature of the His-15 site by resonances which display parallel effects. Resonances at δ 0.41, 1.19, and 1.21 ppm all show the same order of interaction across the set of complexes as does His-15 δ-CH.[33] These chemical shift values correlate well with literature values[28] for Ile-88 γ-CH (0.41 and 1.21 ppm) and Thr-89 γ-CH_3 (δ 1.18 ppm) which are all located near His-15 [distances from His-15 δ-C: 4.6 Å (Ile-88 γ^1-C), 6.9 Å (Ile-88 γ^2-C), and 5.2 Å (Thr-89 γ-C)]. The data appear to imply that the binding interactions involve hydrophobic residues such as Ile-88 located near His-15.

The Leu-84 Weak Site. A stereochemically parallel binding pattern to that observed with resonances associated with the His-15 site appears more weakly in another set of resonances. These appear at δ 1.03, 1.06, 1.74,[33] and 6.9 ppm (Figure 2), and correlate to literature[28] shifts of δ 1.04 (Leu-84 δ-CH_3), 1.74 (Leu-84 γ-CH), 1.06 (Thr-43 γ-CH_3), and 6.83 (Tyr-53 ε-CH). The residues which appear to be involved are clustered just under the active cleft, roughly beneath the catalytic residue Asp-52, with

(30) Kirk, A. D.; Namasivayam, C. *Inorg. Chem.* **1988**, *27*, 1095–1099.
(31) Haupt, G. *J. Res. Natl. Bur. Stand. (U.S.)* **1952**, *48*, 414.
(32) Initial broadening studies also suggested that the probes undergo loss of ~1 imidazole ligand followed by aquation (see ref 24).
(33) Bocarsly, J. R. Ph.D. Thesis, Columbia University, 1989.

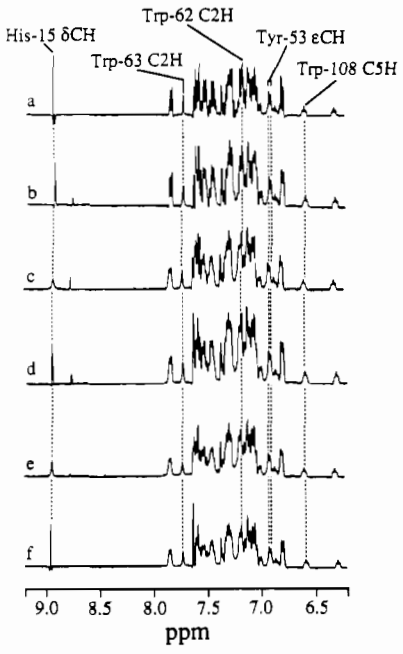

Figure 2. Paramagnetic broadening effects observed in the aromatic region of lysozyme (protein concentration, 3 mM; quencher/protein ratio, 1:5): (a) free protein ^{1}H spectrum; (b)–(f) relaxation effects of **1** (b), **2a** (c), **2b** (d), **3a** (e), **3b** (f).

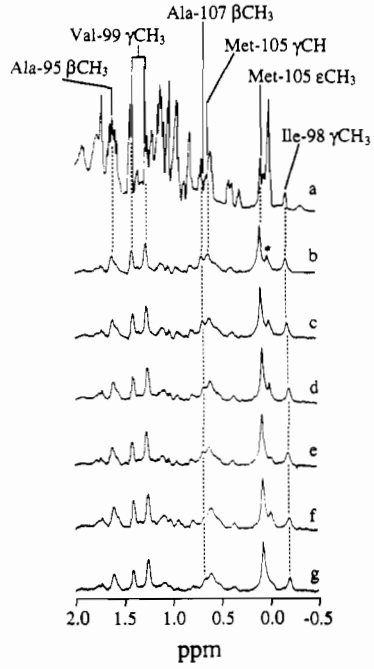

Figure 3. NOE quenching spectra of NOEs produced by irradiation of Trp-108 C5H at δ 6.57 ppm (protein concentration, 3 mM; quencher/protein ratio, 1:5): (a) free protein ^{1}H spectrum; (b) lysozyme free protein NOEs; (c)–(g) relaxation effects of **1** (c), **2a** (d), **2b** (e), **3a** (f), **3b** (g). The starred peak is a subtraction artifact due to the DSS standard.

Thr-43 γ-CH_3 located centrally between Tyr-53 ε-CH and Leu-84 δ-CH_3, and γ-CH. The difference between enantiomers is most noticeable in the Thr-43 and Leu-84 resonances, and is least obvious in the Tyr-53 protons. The chromium center appears to interact with the surface of the protein near the γ-CH_3 of Thr-43 and the Leu-84 δ-CH_3 groups.

The Val-120 Weak Site. There appears to be an interaction common to the entire series of probes which appears in broadened resonances at δ 1.11 and 1.13 ppm.[33] These may be due to the methyl resonances of Val-120, assigned[28] at δ 1.09 and 1.14 ppm. Nearby resonances which may be due to protons involved in the same interaction are at δ 1.21 ppm, which may be the methyl group of Ala-122; however, this is unclear, since the Ile-88 γ-CH resonance is located at the same position.[28] Another resonance which may be related is found at δ 1.28 ppm; this may be due to a Ile-124 γ-CH proton, which is close to Val-120 and Ala-122. Interaction at this site is equal in strength for all the probes.

The Active Cleft Site. The second set of strongly perturbed resonances, which show the same level of effect as the His-15 site, revolve around the β-CH_3 protons of ala-107. This resonance, found at δ 0.67 ppm,[28] is the most strongly affected of those associated with this site. Principally associated with Ala-107 β-CH_3 are the resonances Ile-98 γ-CH_3, Trp-62 C2H, and Trp-63 C2H; less strongly affected are Ile-98 β-CH and Asp-59 β-CH.

NOE Quenching in the Active Cleft. The effect of metal complex interaction at this site can most easily be seen in the NOE quenching spectra of the complexes. Figure 3 illustrates the quenching effects observed: the NOE from Trp-108 C5H to Ala-107 β-CH_3 is strongly quenched while the NOE to Ile-98 γ-CH_3 is moderately affected; NOEs from the same proton to Met-105 γ-CH, Met-105 ε-CH_3, Val-99 γ-CH_3, and Ala-95 β-CH_3 are unaffected. Examination of the NOE quenching efficiency to Ala-107 β-CH_3 as a function of complex structure reveals too that while all of the complexes quench the NOE to Ala-107 β-CH_3, the quenching order **3a** > **3b** ≈ **2a** ≈ **2b** > **1** is found. Relaxation data for complexes **1** and **3a** (the least and most efficient quenchers) are summarized in Table I.

The quenching of the NOE to Ala-107 β-CH_3 has been studied as a function of quencher concentration. The most effective quencher **3a** and the least effective **1** are compared in Figure 4. Consistent with a situation of weak binding, the degree of quenching in both cases increases with quencher concentration. Roughly the same effect is observed for **1** at a protein-to-quencher ratio of 1.25:1 as is seen for **3a** at a ratio of 5:1, indicating that **3a** is about 4 times more efficient than **1**. At a ratio of 2.5:1, **3a** has completely quenched the NOE to Ala-107 β-CH_3; a small residual signal to Ile-98 γ-CH_3 remains. This suggests a closer position of the paramagnetic metal center to the methyl group of Ala-107 than to that of Ile-98.

Table I. Summary of NMR Data for the Active Cleft Binding Region[a]

	NOE quenching			
		NOE enhancements,[b] %		
paramagnetic broadening	proton NOE	free protein	**1**	**3a**
	Binding Region Protons			
Trp-62 C2H	Asn-59 α-CH → Asn-59 β^1-CH	26	20	18
Trp-63 C2H	Asn-59 α-CH → Asn-59 β^2-CH	34	28	25
Ala-107 β-CH_3	Asn-59 α-CH → Trp-62 C2H	13	9	9
	Asn-59 α-CH → Trp-63 C2H	6	4	2
	Asn-59 α-CH → Trp-63 C5H	6	5.5	4
	Ile-98 γ-CH → Ile-98 β-CH_2	53	50	46
	Ile-98 γ-CH → Ile-98 γ-CH_3	65	58	46
	Trp-108 C5H → Ile-98 γ-CH_3	10	9	6
	Trp-108 C5H → Ala-107 β-CH_3	12.4	12	7
	Border Protons			
Asn-59 α-CH	Trp-28 C5H → Leu-56 δ^1-CH_3			
Trp-108 C5H	Trp-28 C5H → Leu-56 δ^2-CH_3			
Ala-110 β-CH_3	Trp-28 C5H → Ala-95 β-CH_3			
	Trp-108 C5H → Trp-108 C4H			
	Trp-108 C5H → Trp-108 C6H			
	Ile-98 γ-CH → Ile-98 δ-CH_3			

[a] NOEs are listed with the irradiated resonance to the left of the arrow. Selected NOE enhancements for the free protein and protein in the presence of quenchers **1** and **3a** are presented in the right-hand column. [b] NOE enhancements are defined percentages calculated from the integrated peak area ratios of NOE peak to irradiated peak.

Other NOE quenching experiments which shed light on the active cleft site are those from Ile-98 γ-CH to the other protons on Ile-98.[33] As one travels along the Ile-98 carbon framework away from Ala-107 toward the other Ile-98 carbons, the quenching effect attenuates. This confirms that the chromium center is generally located in between Ala-107 β-CH and Ile-98 γ-CH_3, and closer to Ala-107, where the largest effect is observed. NOEs

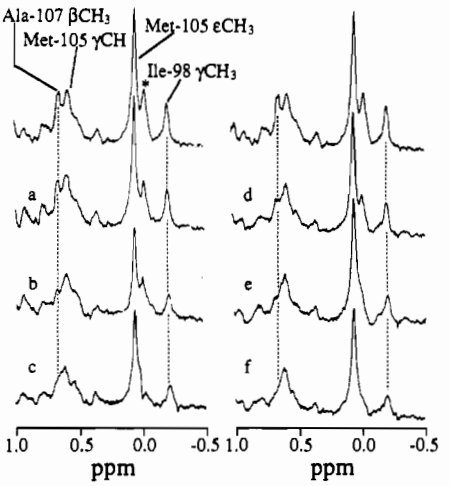

Figure 4. NOE quenching as a function of quencher to protein ratio by **1** (left panel) and **3a** (right panel). The top spectrum in each panel is free lysozyme NOEs. Quencher to protein ratios: (a) 1:5; (b) 1:2.5; (c) 1:1.25; (d) 1:10; (e) 1:5; (f) 1:2.5. All protein concentrations are 3 mM. The starred peak is a subtraction artifact due to the DSS standard.

from Asn-59 α-CH to three aromatic protons (Trp-62 C2H, Trp-63 C2H and Trp63 C5H) are also informative. The quenching effects at these resonances range in the order Trp-63 C2H > Trp-62 C2H > Trp-63 C5H, suggesting that the metal center is located closest to Trp-63 C2H, and on the C2 (as opposed to the C5) side of the indole rings. NOEs from Asn-59 α-CH to the Asn-59 β-CH_2 protons exhibit moderate quenching. The NOEs quenched by metal complex binding involve protons which form a radial distribution about subbinding site C in the lysozyme active cleft.

The terminus of the binding region can be further delimited by focusing on protons that are in close proximity to the most weakly affected protons; those that show no effect define the border of the binding region. The border protons identified are listed in Table I. The positions of these protons are fully consistent with the radial quenching distribution about subsite C. In addition, no broadening effect is seen at Asp-52 α-CH (δ 5.25 ppm) or Gln-57 β-CH_2 (δ 2.03 and 2.15 ppm), located in subsites D and E of the active cleft, suggesting that binding is limited specifically to the region around subsite C.

The NOE quenching results presented above complement the effects seen in the paramagnetic broadening spectra.[33] The most efficient case of NOE quenching, involving the NOE from Trp-108 C5H to Ala-107 β-CH_3, shows a very significant broadening effect at the Ala-107 β-CH_3 resonance. Other resonances which show the same behavior in both the NOE quenching and the broadening experiments are those due to Trp-62 C2H and Trp-63 C2H. The broadening effects at these resonances also exhibit the same efficiency pattern as observed in the NOE quenching data.

Covalent Labeling Reactions of 1 with Lysozyme. As can be seen in Figure 5, CD signal builds up as a function of the reaction time of **1** with lysozyme (Figure 5a) or as a function of the increasing ratio of metal complex to protein at constant time.[33] In an effort to determine whether the site of labeling can be controlled through pH, labeling reactions were run at a variety of pH values. Results similar, but not identical, to those appearing in Figure 5a (pH 5) were obtained at pH 6 and 7. Experiments run at pH 4 under the conditions of the NMR studies described above (35 °C, ~2 h) produced no CD signal, verifying that no covalent labeling occurs under the NMR conditions used.[33]

The differences in CD spectra of reactions run at pHs in the range 5–7 amount to an increase in intensity of the positive band at 512 nm (observed at lower pH), and a slight blue shift in the negative peak at 410 nm.[33] This effect does not appear to indicate a difference in the type of coordinated residue, as the overall features of the spectrum are maintained; however, it does appear to be indicative of some change in the metal coordination sphere. To understand the origins of the differences in the CD spectra,

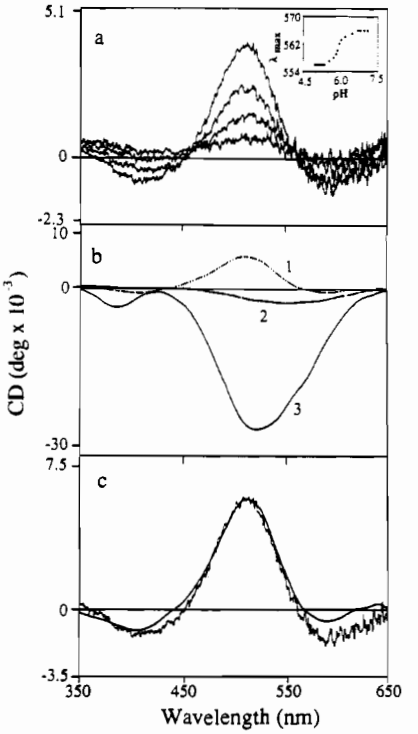

Figure 5. (a) CD spectra taken during the reaction of **1** with lysozyme: reaction as a function of time at pH 5, 4.4 mM lysozyme, 0.9 mM **1**, where spectra were taken after 60, 120, 180, and 240 min of reaction (the inset shows the pH titration of lysozyme labeled with **1**, followed by a blue shift in λ_{max} of the low-energy peak). (b) CD spectra of covalent binding site models of **1** to lysozyme side chains: spectrum 1, **1a**; spectrum 2, **1b**; spectrum 3, **1c**. All concentrations were adjusted to 5 mM. (c) Comparison of CD spectra of lysozyme labeled at pH 5 with that of **1a**. The spectrum of **1a** is from part b with the ordinate axis adjusted for comparison.

labeled protein was titrated over the pH range 7.6–4.6 with $HClO_4$. The changes during titration parallel those seen in the spectra of protein labeled at pH 5 vs pH 7. Concomitant changes in the visible spectrum occur, including a 10-nm blue shift of the low-energy d–d band. A plot of λ_{max} of this peak vs pH produces a sigmoidal curve with an equivalence point at pH $\approx$ 5.9 (inset, Figure 5a).

Protein–Metal Stoichiometry. The metal concentration of a volumetric solution of fully labeled lysozyme was determined by atomic absorption, and the spectroscopic parameters of the metal chromophores, as well as the metal binding stoichiometry, were determined on this basis. The metal:protein stoichiometry was determined to be 2.9:1 using a protein molecular weight corrected for the mass of the transition-metal labels. The spectroscopic parameters determined (both visible and CD) for the protein–metal complex represent an average of the parameters for the three coordinated labels. Typical values (at pH 7) are $\Delta\epsilon_{512}$ = +0.34 M^{-1} cm^{-1}, $\Delta\epsilon_{410}$ = –0.11 M^{-1} cm^{-1}, ϵ_{566} = 69 M^{-1} cm^{-1}, and ϵ_{405} = 87 M^{-1} cm^{-1} (the inverse molarity of chromium is used in the units).

Model Reactions of 1 with Protected Amino Acids. Models of the possible covalent binding sites on lysozyme were synthesized by the reaction of **1** with appropriate amino acids. Possible donor groups on lysozyme with sufficient solvent accessibility to coordinate include one leucine carboxylate (at the carboxy terminus), one histidine, six tryptophan, seven aspartic acid, and two glutamic acid residues. These amino acids in protected form were reacted with **1**. The carboxylate-containing amino acids produced monosubstituted derivatives **1a–c**. Reaction with histidine resulted in the formation of a chelate.[33] No measurable reaction occurred with tryptophan.

The carboxylate-coordinating amino acids (Leu, Asp, and Glu) react as expected with **1**, according to eq 1:

$$\mathbf{1} + \mathrm{RCOOH} \rightarrow [\mathrm{Cr(NTA)(Im)(RCOO)}]^- + \mathrm{ImH}^+ \quad (1)$$

Table II. Extinction Coefficients (ϵ) and Molar Circular Dichroism ($\Delta\epsilon$) for Complexes **1**[a]

	band 1		band 2	
complex	abs $\lambda_{max}(\epsilon)$	CD $\lambda_{max}(\Delta\epsilon)$	abs $\lambda_{max}(\epsilon)$	CD $\lambda_{max}(\Delta\epsilon)$
$Cr(NTA)(Im)_2$ (**1**)	535 (95)		390 (126)	
Cr(NTA)(Im)(Asp) (**1a**)	555 (94)	513 (+0.035) 591 (−0.004)	403 (104)	408 (−0.006)
Cr(NTA)(Im)(Glu) (**1b**)	558 (102)	552 (−0.016)	403 (114)	
Cr(NTA)(Im)(Leu) (**1c**)	545 (95)	524 (−0.080), 576 (sh)	399 (111)	388 (−0.011)
Cr(NTA)(His-N,O)[b]	549 (105)	508 (−0.096) 569 (+0.090)	546 (110)	407 (+0.060)

[a] Values calculated on the basis of chromium concentrations obtained by alkaline oxidation of the complexes by hydrogen peroxide to chromate ion. Units: λ, nm; ϵ and $\Delta\epsilon$, M^{-1} cm^{-1}. [b] His-N,O denotes bidentate coordination through both the imidazole nitrogen and the carboxylate oxygen.

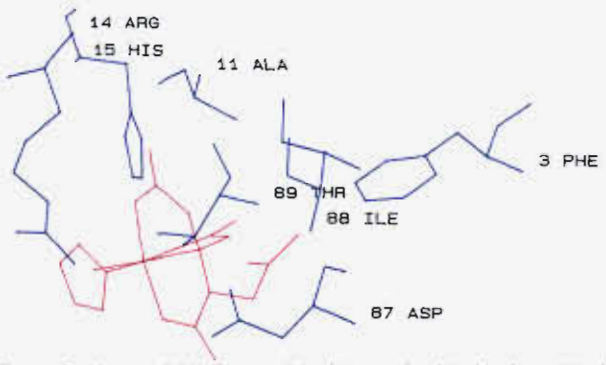

Figure 6. Proposed binding model of **2a** at the His-15 site, with the relevant protein residues shown in blue and the metal complex in red. Possible hydrogen bonds to His-15 imidazole NH and the NH of Ile-88 may help orient the complex. This orientation allows the leucine side chain to sit in the hydrophobic region defined in part by Ala-11 and Ile-88.

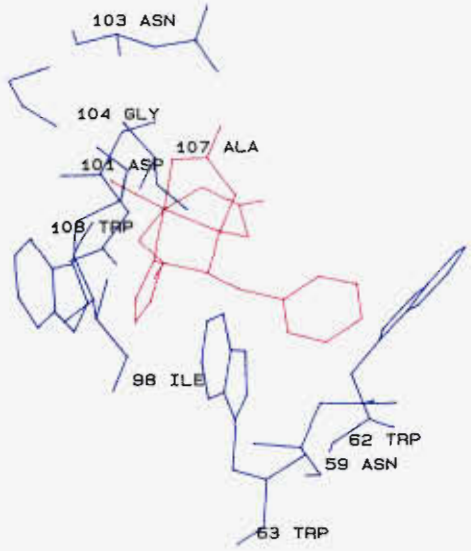

Figure 7. Proposed binding model of **3a** at the active cleft site, with the relevant protein residues shown in blue and the metal complex in red. The proposed interactions, including hydrogen bonds to the carboxylate of Asp-101 (which should be largely protonated at the experimental pH[26]), the amide group of Asn-103, and the peptide carbonyl of Gly-104 and an aromatic–aromatic interaction between the pendant phenylalanine side chain of **3a** and Trp-62 and/or Trp-63, impose an orientation on the molecule which places the chromium center in close proximity to the methyl group of Ala-107.

The positive and negative ion FAB spectra of the products indicate that all of the complexes contain a single Cr(NTA) moiety, a single imidazole, and a single protected amino acid.[34] On the basis of ^2H NMR studies of the aquation of **1**, the imidazole trans to the amine nitrogen leaves most readily and is the likely site of substitution.[24]

As a spectroscopic probe for the type of amino acid ligand, the CD spectra of the model complexes were measured (Figure 5b and Table II). While complex **1** itself is achiral, the model complexes **1a–c** are dissymmetric, by virtue of the chiral carbon on each coordinated amino acid. The rotational strength due to its vicinal dissymmetry is known to be dependent on the distance between the chiral center and the chromophore.[20] In addition, there is an inversion of sign of the Cotton effect on increasing number of bonds between chiral center and chromophore, a characteristic of such systems.[35,36] The result of these effects is to produce a discrete CD signature for each type of coordinated amino acid, which can be used to establish the residue involved in coordination of **1** to the protein.

Discussion

Figure 1 summarizes the various sites of association of the metal complexes with the protein surface based upon the NOE quenching and CD spectroscopic results. Figures 6 and 7 show more detailed structural models of the aquated chromium complex bound in each of the two major binding sites based upon the NMR results. The combined NMR data as a function of side chain substitution on the metal complex permit a specific delineation of the orientation and interactions of the metal complexes on the protein surface. Moreover, the CD results, which describe sites of covalent modification, indicate a correspondence with and indeed even an influence of the noncovalent binding interactions in directing labeling.

The His-15 Site. A proposed binding model is presented in Figure 6 which is based upon the NOE quenching and the ordering of metal complex binding effects observed (**2a** ≈ **3a** > **1** > **2b** ≈ **3b**). The interaction at the His-15 site is likely due to hydrogen bonds formed between the ligand hydrogen-bonding groups and the protein. The structure-dependent broadening effects observed at the His-15 site indicate that the interaction is affected only by the position of the side chain with respect to the other moieties on the complex, since binding differences depend on side chain stereochemistry and not on the type of side chain. Given the side chains used, this exclusive dependence on stereochemistry also implies that a hydrophobic effect governs binding.[37] Nonpolar residues near His-15, such as Ile-88 and Ala-11 (~5 Å and 5.7 Å from His-15 δ-C) may provide such a hydrophobic environment. The broadening observed at Ile-88 would appear to support this

(34) The positive ion FAB spectra in methanolic 50 mM LiBr for **1a–c** all contain a peak corresponding to the mass of the parent ion plus two positively charged ions (either H^+ or Li^+). This is seen as indicating that the negatively charged product acquires two positively charged ions (H^+ or Li^+) for an overall single positive charge. See, for example, Cerny, R. L.; Gross, M. L. *Anal. Chem.* **1985**, *57*, 1160–1163. Puzo, G.; Prome, J. C.; Macquet, J. P.; Lewis, I. A. S. *Biomed. Mass Spectrom.* **1982**, *9*, 552–556. Significant observed m/e ratios are (positive ion) $(m + 7 + 7)^+ = 644$ (**1a**), 658 (**1b**), 552 (**1c**); $(m + 7 + 7)^+ - 68 = 576$ (**1a**), 590 (**1b**), 484 (**1c**); (negative ion): $(m^- - 68)^- = 562$ (**1a**), 576 (**1b**), 470 (**1c**).

(35) Djerassi, C.; Geller, L. E. *J. Am. Chem. Soc.* **1959**, *81*, 2789–2794.

(36) Diener, W.; Frelek, J.; Gerards, M.; Majer, Z.; Perkowska, A.; Snatzke, G.; Vlahov, I.; Wagner, U. *F.E.C.S. Int. Conf. Circ. Dichroism, Conf. Proc.*, Sept. 21–25, 1985; Bulgarian Academy of Sciences, 1985; Vol. 6, pp 11–33.

(37) Standard hydrophobicity scales place leucine and phenylalanine close to each other in hydrophobicity. See: Tanford, C. *J. Am. Chem. Soc.* **1962**, *84*, 4240–4247. Nozaki, Y.; Tanford, C. *J. Biol. Chem.* **1971**, *246*, 2211–2217. Bull, H. B.; Breese, K. *Arch. Biochem. Biophys.* **1974**, *161*, 665–670.

notion. Other candidates for constituents of a hydrophobic pocket near His-15 include the side chains of Val-92, Met-12, and Phe-3, which all approach within 8 Å of His-15 δ-C. Previous lysozyme studies support the idea of a hydrophobic binding pocket in this region.[38-40]

These considerations suggest that the complexes bind relatively close to His-15 via hydrogen bonding, which allows the side chains of appropriate stereochemistry to sit in the bottom of the hydrophobic pocket; in complexes of opposite stereochemistry, the side chain is forced out toward the solution, disfavoring binding. The unsubstituted parent complex **1**, while it cannot take advantage of hydrophobic effects, can still attain the level of binding provided by the unsubstituted molecular framework.

The Active Cleft Site. The NOE quenching results, as supported by broadening experiments, provide an extremely clear picture of the active cleft binding by the complexes **1–3** in which the largest perturbations in the NMR spectra are seen at Ala-107, with the effect weakening as one travels radially outward from Ala-107 toward Ile-98, Trp-63, Trp-62, and Asn-59. The pattern suggests that the paramagnetic center is located closest to Ala-107 β-CH_3, and roughly in between Ala-107 β-CH_3, Ile-98 γ-CH_3, and Trp-63 C2H.

There remains, however, an additional aspect to the binding of complexes **1–3** to the active cleft site. As demonstrated in Figure 3, both the type of side chain and its stereochemistry affect binding, resulting in quenching efficiencies in the order **3a** > **3b** ≈ **2a** ≈ **2b** > **1**. Given the nature of the side chains involved, hydrophobicity almost certainly plays a role in the degree of binding of the substituted complexes. Certainly, hydrophobicity is most likely the explanation for the increased binding of **2a,b** over **1**, as a relatively nonpolar environment for an alkyl side chain may be provided by several of the residues involved in the binding region, which include isoleucine and tryptophan.

Hydrophobicity by itself, however, may not be sufficient to explain the behavior of **3a**, whose side chain is approximately equal to the leucine side chain in hydrophobicity[37] and exceeds the leucine group in steric bulk, yet facilitates greater quenching than the leucine group. The increase in effect by **3a** over the other members of the series may be due to an aromatic–aromatic interaction between the pendant phenylalanine side chain and either one or both of the aromatic systems in the binding region (Trp-62 and Trp-63). Such aromatic–aromatic interactions have been noted in studies of protein X-ray structure data bases.[41,42] The free energy of these interactions has been calculated to be in the 1–2 kcal/mol range.[43] Most significant for this study, aromatic–aromatic interactions have also been observed between bound substrates and side chain groups in their binding sites.[44,45]

Apropos of this proposal, the phenylalanine side chains of **3a** have been demonstrated to be competent to participate in aromatic–aromatic interactions. These interactions have been characterized in the crystal structure of **3a**, in which the side chain rings interact in the appropriate geometry with each other as well as with toluene molecules of crystallization.[24] Therefore, it appears likely that the explanation of the difference in quenching efficiency between **3a** and **2a,b** lies in the formation of nonclassical aromatic–aromatic interactions between the metal complex side chain and suitable protein moieties. Along these lines, it seems that the relative equivalence in quenching efficiency between **2a,b** and **3b** is explained by the stereochemistry of **3b**; the position of the aromatic ring is apparently inappropriate for interaction with protein aromatic groups, so hydrophobic effects roughly equivalent to those in **2a** and **2b** dominate. Our proposed binding model at the active cleft site for complex **3a** is depicted in Figure 7.

While we have proceeded on the assumption that the differences in relaxation efficiency observed between complexes of different structure are due to differences in binding, these effects may be due either to a higher binding constant of the metal complex at a given site or to a change in relative positioning of a paramagnetic transition-metal ion in the complex to the involved proton. In the case of the active cleft binding region, however, where the metal complexes interact with several protons (Ala-107 β-CH_3, Ile-98 γ^2-CH_3, Trp-63 C2H, Trp-62 C2H, Asn-59 β^1-CH, Asn-59 β^2-CH) radially distributed about the putative binding location, the nature of the effect may be assessed. Given the radial distribution around the chromium center of affected protons, if a change in binding mode brought the metal center closer to a particular proton and caused an increase in quenching, then a *decrease* in quenching should be observed for other protons in the binding region, as movement of the complex's average position toward one proton must result in its movement away from others. If, on the other hand, an increase in quenching of a particular proton by a specific complex is due to a higher binding constant for that complex, then all the affected protons in the binding region should show the increase. The NOE quenching data indicate that, where an increase in quenching of one complex as compared to another occurs, increased quenching at all affected protons is observed, suggesting that the quenching differences of the substituted analogues of **1** are due to higher binding constants (Table I). The same may be said of the resonances at the His-15 site which are broadened; however, lack of a set of resonances with a large enough radial distribution at this site makes this conclusion somewhat more tenuous.

Covalent Labeling of Lysozyme. The formation of a CD spectrum as a function of the reaction time of nondissymmetric **1** with lysozyme provides clear evidence for the formation of covalent bonds between metal complex and protein side chains. The existence of such bonds is confirmed by the stability of the dissymmetric chromophore to equilibrium dialysis. The CD signal has identical peaks at all reaction times and metal complex to protein ratios suggesting that the same sites are labeled in all cases; no less-reactive sites are found at the forcing condition of higher ratios. It was hoped that the location of the transition-metal tag could be manipulated by pH; however, at all accessible pH values (pH 5–7), similar CD spectra are produced, suggesting that the labeling sites do not change in this range.

Titration of the bound complex (inset, Figure 5a) shows that a proton is lost from the chromophore at pH ≈ 5.9. The identity of this value with the pK_a of the aquo ligand in $Cr(NTA)(H_2O)_2$ (pK_a = 5.87[46]) suggests that the protein-bound complex acquires an aquo ligand in its sixth coordination site. This is consistent with the aquation chemistry of **1** in this pH range, in which aquation at the imidazole sites occurs in two successive steps, and appears to be followed by proton loss and μ-dihydroxy dimer formation.[24] Given a labeling stoichiometry of 3:1, the titration curve represents the average of the pK_as of the aquo ligand on all three $Cr(NTA)(H_2O)(lysozyme)_{1/3}$ complexes. The narrowness of this transition suggests that the three pK_as are relatively close to each other. This implies that the environments of the three chromium labels are similar, and furthermore, that all three are coordinated to highly exposed groups, since the pK_as are indistinguishable from that of the free label.

The likely coordinating groups on the protein surface are either carboxylate or imidazole side chains. There are no sulfur-containing residues with sufficient solvent accessibility to coordinate. While there are exposed tryptophan moieties, it has been reported that tryptophan residues in specific proteins[5] and peptides[47] are poor ligands, and the failure of tryptophan to react with **1** in the model complex synthesis adds further support to this observation.

(38) Yamada, H.; Uozumi, F.; Ishikawa, A.; Imoto, T. *J. Biochem.* (*Tokyo*) **1984**, *95*, 503–510.
(39) Ueda, T.; Yamada, H.; Hirata, M.; Imoto, T. *Biochemistry* **1985**, *24*, 6316–6322.
(40) Piszkiewicz, D.; Bruice, T. C. *Biochemistry* **1968**, *7*, 3037–3047.
(41) Singh, J.; Thornton, J. M. *FEBS Lett.* **1985**, *191*, 1–6.
(42) Burley, S. K.; Petsko, G. *J. Am. Chem. Soc.* **1986**, *108*, 7995–8001.
(43) Burley, S. K.; Petsko, G. *Science* **1985**, *229*, 23–28.
(44) Ringe, D. B.; Seaton, D. B.; Gelb, M.; Abeles, R. H. *Biochemistry* **1985**, *24*, 64–68.
(45) Lipscomb, W. N. *Proc. R. A. Welch Found. Conf. Chem. Res.* **1971**, *15*, 140.
(46) Irving, H. M. N. H.; Al-jarrah, R. H. *Anal. Chim. Acta* **1972**, *60*, 345–355.
(47) Smith, M. C.; Furman, T. C.; Ingolia, T. D.; Pidgeon, C. *J. Biol. Chem.* **1988**, *263*, 7211–7215.

Table III. Exposure Ratio Values[a] of Relevant Amino Acid Side Chains for HEW Lysozyme[26]

residue	exposure ratio	residue	exposure ratio	residue	exposure ratio
Asp-18	0.3	Asp-87	0.7	Glu-35	0.2
Asp-48	0.3	Asp-101	0.8	Leu-129	0.7
Asp-52	0.3	Asp-119	0.5	His-15	0.2
Asp-66	0.0	Glu-7	0.4		

[a] Calculated by comparing the crystallographically determined van der Waals surfaces of a given side chain in the folded protein with the that found in a model peptide containing the same residue.

The labeled residues may be identified by a comparison between the CD spectra of labeled protein with those of the model complexes (Figure 5b). As Figure 5c illustrates, there is an excellent correspondence between the CD of **1a** and the spectrum of the labeled protein. The positive Cotton effect at 512 nm is reproduced nicely in the model complex spectrum, as is the small negative effect at 410 nm (without replacement of the imidazole in the sixth coordination site, which causes only minor perturbations in the CD).[33] This comparison suggests that all three labeled sites are aspartic acid residues. Also suggestive is the fact that, of the seven aspartic acid groups in the protein, only three have relatively high solvent accessibilities (Asp-87, Asp-101, and Asp-119). Either low solvent exposure or the instability of the Cr(III)–histidine bond toward aquation[48] may explain why no labeling at the histidine imidazole occurs. Table III contains lysozyme exposure ratios for all relevant groups.[26]

Relationship between Sites of Noncovalent Interaction and Positions of Covalent Labeling. The comparison afforded by the exposure ratio values of the aspartic acid residues to the other carboxylate-containing amino acids also points to the effect of noncovalent association on covalent labeling. Given that there are residues which have roughly comparable solvent accessibilities to the aspartic acid groups thought to be involved in this reaction (e.g., Leu-129 and possibly Glu-7), the question arises of why labeling occurs exclusively at aspartic acid, and not at other carboxylates (which should have similar reactivity). One intriguing explanation is that the sites of covalent binding are influenced by the noncovalent associations, as elucidated by NMR techniques. The three aspartic acid groups implicated as covalent binding sites all are located near or within the noncovalent binding regions (Figure 1). In the active cleft site, Asp-101 is found 4.2 Å from Ile-98 γ^2-CH_3 and may form a hydrogen bond with a ligand carboxylate. At the His-15 site, Asp-87 is located 4.8 Å from N3 of the imidazole ring of His-15. Finally, Asp-119 is in close proximity to Val-120, which appears to be a minor sight of interaction, although the characterization of this third noncovalent site is the most doubtful. Thus, metal complex labeling appears to occur specifically at carboxylates which are appropriately located near the sites of noncovalent binding, and not at equally exposed carboxylates which are distant from noncovalent sites. This suggests that the noncovalent interactions of the complexes exert an influence over the coordination sites of the complexes on the protein surface.

Conclusion. This work presents new approaches designed to elucidate sites of binding, both covalent and noncovalent, of small metal complexes to proteins. These techniques provide sensitive methods to characterize structurally subtle molecular interactions in solution. Weak noncovalent interactions have been studied by the methods of nuclear Overhauser effect quenching and paramagnetic broadening experiments, leading to the identification of four sites of interaction between the complexes **1–3** and HEW lysozyme. Information about binding mode, in addition to location, has also been obtained by an examination of the effects of substituents on the metal chelate rings. These substitutions, which may be regarded as a variable set of recognition elements, are shown to affect the ordering of the level of interaction of **1–3** at different sites, which may be reflective of differing interactions at the various sites. Specifically, the data have been interpreted in terms of hydrophobic effects at the His-15 site, and both hydrophobic and aromatic–aromatic interactions at the active cleft site. In addition, the covalent binding of these complexes to protein surface groups has been studied using CD spectroscopy. The utility of CD spectroscopy to identify the type of amino acid side chain involved in protein labeling via vicinal dissymmetry induced by the coordinated side chain to the metal complex has been demonstrated. Moreover, a comparison of binding interactions via the two modes versus solvent accessibility of differing residues leads to the notion that the sites of noncovalent interaction between metal complex and protein surface appear to play an influential role in directing the metal coordination to the macromolecule.

Acknowledgment. We express our gratitude to Dr. Christopher Turner for his assistance with the NMR experiments. In addition, we are grateful to the NIH (Grant GM 33309) for their financial support.

Registry No. **1**, 123266-17-1; **1a**, 141375-99-7; **1b**, 141376-00-3; **1c**, 141376-01-4; **2a**, 141376-02-5; **2b**, 130694-22-3; **3a**, 123266-18-2; **3b**, 130694-23-4.

(48) Winter, J. A.; Caruso, D.; Shepherd, R. E. *Inorg. Chem.* **1988**, *27*, 1086–1089.